

Alginate-PEG Sponge Architecture and Role in the Design of Insulin Release Dressings

Michael Hrynyk,[†] Manuela Martins-Green,[‡] Annelise E. Barron,[§] and Ronald J. Neufeld^{*,†}

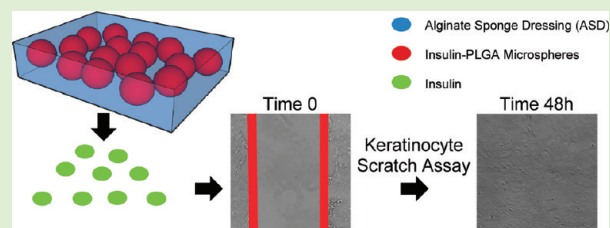
[†]Department of Chemical Engineering, Queen's University, Kingston, Ontario, Canada K7L 3N6

[‡]Department of Cell Biology and Neuroscience, University of California—Riverside, Riverside, California 92521, United States

[§]Department of Bioengineering, Stanford University, Stanford, California 94305, United States

S Supporting Information

ABSTRACT: Wound healing is a natural process involving several signaling molecules and cell types over a significant period of time. Although current dressings help to protect the wound from debris or infection, they do little in accelerating the healing process. Insulin has been shown to stimulate the healing of damaged skin. We have developed an alginate sponge dressing (ASD) that forms a hydrogel capable of providing a moist and protective healing environment. By incorporating insulin-loaded poly(D,L-lactide-co-glycolide) (PLGA) microparticles into ASD, we successfully stabilized and released insulin for up to 21 days. Insulin release and water absorption and transfer through the ASD were influenced by altering the levels of poly(ethylene glycol) (PEG) in the dressing matrix. Bioactivity of released insulin can be maintained for at least 10 days, demonstrated using a human keratinocyte migration assay. Results showed that insulin-loaded PLGA microparticles, embedded within PEG-ASD, functioned as an effective long-term delivery platform for bioactive insulin.



INTRODUCTION

Skin is a continuous living organ offering a protective function for internal tissues and organs. Injury from exposure to heat, chemicals, or abrasion can compromise skin integrity, exposing the body to blood loss and possible infection.¹ Depending on the size and extent of the wound, intervention in addition to the natural healing process is often necessary.² Wound dressings facilitate wound closure and repair by acting as a temporary barrier to microorganisms and debris and to moisture loss.^{3–5} This passive function is often sufficient, but available wound dressings do not offer a stimulatory function often needed to promote the rate of wound healing and, thus, minimize the recovery period.

Growth factors such as epidermal (EGF), transforming factor beta (TGF- β), and platelet derived growth factor (PDGF) have been shown to be effective in wound healing,^{6–8} but high cost (\$1500–10000 USD per mg),⁹ poor stability, and lack of controlled release vehicles have prevented application.

Insulin is one alternative which was first recognized to accelerate wound healing in the late 1920s.¹⁰ Several decades later, Rosenthal (1968) and Udupa et al. (1971) reported increased wound tensile strength, decreased wound healing times, and denser and more aligned collagen fibers in rats treated with topically applied insulin.^{11,12} Topical insulin application to excision wounds in mice has also lead to accelerated re-epithelialization, by stimulating angiogenesis and increasing blood vessel stability, as well as promoting a higher level of maturation of the healing tissues.¹³ Commercially, insulin is also available at a cost of less than \$1 USD/mg, therefore, serving as a far more cost-effective biotherapeutic, as

well as a more stable alternative to other growth promoting proteins.

Previously, sustained release of bioactive insulin from poly(D,L-lactic-co-glycolic acid) (PLGA) microspheres was demonstrated for up to 25 days.¹⁴ Although this encapsulation polymer provided an effective means of stabilizing and releasing insulin, it was necessary to develop an approach for distributing insulin across a wound via a controlled release, biocompatible dressing.

Alginates are polysaccharides composed of alternating mannuronic (M) and guluronic (G) acid moieties and have been used in wound dressings for decades.¹⁵ As a wound dressing matrix, alginate hydrogels are highly biocompatible, provide excellent hemostatic control, are able to absorb large quantities of wound exudate, and can be easily and painlessly removed.^{16–18} Furthermore, the incorporation of poly(ethylene glycol) (PEG) can also help to preserve peptide bioactivity and attenuate release kinetics.¹⁹ Given that the list of favorable attributes of alginates and PEGs are complementary, the combination of alginate and PEG could be used as a novel basis for a next generation composite wound dressing.

Thus the objective of this study was to incorporate insulin-loaded PLGA microspheres into alginate-PEG sponge dressings that can be applied to wounds, and are practical for development, manufacture, and widespread translation to patient populations such as burn victims. High mannuronic

Received: February 2, 2012

Revised: April 11, 2012

Published: April 16, 2012

(M) and high guluronic (G) alginates were utilized at different concentrations, along with variously sized PEGs in designing the dressing material. The effect of formulation on physical properties of the dressing, insulin release kinetics and insulin bioactivity were examined to determine if alginate sponge dressing (ASD) could provide a sustainable platform for enhanced tissue recovery. The results show that a low-density, high mannuronic alginate-PEG sponge dressing, containing insulin-loaded PLGA microparticles is an effective platform for the topical delivery of bioactive insulin and has the potential to promote wound healing.

■ EXPERIMENTAL SECTION

Materials. Human recombinant crystalline insulin (hRcI), poly(ethylene glycol) (PEG) (avg MW 1450 Da and 10 kDa), poly(vinyl alcohol) (PVA) (avg MW 13–23 kDa), CaCl_2 , NaCl, NaOH, and sodium dodecyl sulfate (SDS) were supplied by Sigma Aldrich (Oakville, Canada). Purasorb 5002 PLGA (D,L; 50:50, avg 17 kDa) was obtained from Purac Biomaterials (Lincolnshire, U.S.A.). Dichloromethane (DCM) was supplied by Caledon Laboratories (Georgetown, Canada). Protanal LF10/60 (65–75% guluronic/25–35% mannuronic; G) and LF10/60 LS (35–45% guluronic/55–65% mannuronic; M) were obtained from FMC Biopolymer (Philadelphia, U.S.A.). A Micro BCA protein assay kit was obtained through ThermoFisher (Ottawa, Canada). Human keratinocytes (HaCaT) were purchased from Cell Line Services (Germany). Dulbecco's modified Eagle's medium (DMEM), Dulbecco's phosphate buffered saline (DPBS), and 0.25% trypsin with EDTA were obtained through Gibco (Carlsbad, U.S.A.). Fetal bovine serum (FBS) and penicillin–streptomycin were purchased from Hyclone (Fair Lawn, U.S.A.). Human insulin ELISA kit was supplied by Mercodia (Winston Salem, U.S.A.).

Microparticle Preparation. Microencapsulation of crystalline insulin was performed using a solid-in-oil-in-water (S/O/W) formulation technique previously described.¹⁴ Briefly, insulin-loaded PLGA microparticles were prepared by dissolving 95 mg PLGA into 1 mL of DCM. Crystalline insulin (5 mg) was added to the polymer solution and the suspension was then mixed several times with a Pasteur pipet. The insulin–polymer suspension was added dropwise into an aqueous solution of 5% PVA chilled in an ice bath. The resulting S/O/W emulsion was stirred for 1 min at 430 rpm with an overhead, high shear mixer (Cafra; Warton, Canada). The emulsion was then quickly transferred into a beaker containing 400 mL of distilled water chilled to 5–7 °C and stirred overnight in an ice bath at 200 rpm using a low shear mixer. The hardened microparticles were collected by vacuum filtration, rinsed 3 times with ice cold distilled water and placed into a –20 °C freezer overnight. The microparticles were then transferred into a 4 °C refrigerator for 12 h. Microspheres were stored at –20 °C when not in use.

Alginate Sponge Dressing. Aqueous alginate solutions (2 and 4% w/v) were prepared by slowly adding alginate M (high mannuronic content) or G (high guluronic content) powder into 100 mL of distilled water, under high shear mixing. Various quantities of PEG (0.1–10% w/w) with differing molecular weights (1.45 or 10 kDa) were added to 2% M alginate solutions during the mixing process. Once all of the constituents were fully dissolved, 0.9 mL were transferred into 24-well plates (Costar; Lowell, U.S.A.). Insulin-loaded PLGA microparticles (5 mg) were then directly deposited into the wells and mixed briefly. The plates were frozen at –80 °C for 1 h, then freeze-dried (Virtis; Gardiner, U.S.A.). Circular alginate sponge dressings (ASD) made from high guluronic alginate (G-ASD), high mannuronic alginate (M-ASD), and PEG-high mannuronic alginate (P/M-ASD) were then removed and stored at –20 °C until use.

Microencapsulation Efficiency. Approximately 8–10 mg insulin-loaded microparticles were dissolved into 1 mL of DCM. After full evaporation of the DCM, 10 mL of an aqueous 5% SDS, 0.1 M NaOH solution was added to a vial and stirred for 24 h at 80 rpm with magnetic stir bar while in a 37 °C water bath. Insulin concentration

was measured by a micro BCA protein assay and read spectrophotometrically at 562 nm. Encapsulation efficiencies were expressed as a ratio of the residual insulin versus the insulin added during microencapsulation.

Scanning Electron Microscopy. External and internal morphologies of the various ASD formulations were characterized using SEM (JEOL 840, U.S.A.). Cross sections were prepared by cutting the circular dressings using a razor blade and mounting sections on aluminum stubs covered with double-sided carbon tape. All stubs were gold sputter coated and analyzed.

Physical Properties: Dressing Density. The density of the various ASD was calculated by measuring the dimensions of the circular sample and the mass (Mettler; Mississauga, Canada). The density was expressed as the ratio between the mass and its volume.

Physical Properties: Tensile Testing. The tensile strength of the various ASD was tested by cutting samples into 5 × 20 mm rectangular strips. The dimensions were measured using a digital micrometer prior to attachment to the instrument. The maximum stress (MPa), Young's modulus (MPa), and elongation at fracture were obtained using a texture analyzer (TA Instruments, New Castle, U.S.A.) with a strain of 2 mm/min.

Physical Properties: Water Vapor Transmission Rate. The water vapor transmission rate (WVTR) was determined using a method described in ASTM E96.^{20,21} ASD with a diameter of 15.5 mm was attached using silicone sealant (GE, Huntsville, U.S.A.) to the underside of an inverted netwell insert (Corning; Lowell, U.S.A.), adhered to a polystyrene Petri dish lid. The chamber within the netwell insert was filled with 8 mL of distilled water, and the entire apparatus was placed into an incubator at 35 °C to mimic human skin temperature and a relative humidity of 33%. The mass of the apparatus was weighed at regular intervals to measure the water weight loss over 24 h. $\text{WVTR} = W/(A \times t)$, where W is the weight lost through the membrane, A is the area of the membrane, and t is fixed at 24 h.

Physical Properties: Water Absorption Capacity. The water absorption capacity (WAC) of the ASD was tested using a method modified from that described in the British Pharmacopoeia (BP) monograph for alginate wound dressings and packings.²² Individual ASD were weighed (W_1) and placed in plastic weigh boats filled with (BP) solution A (142 mM NaCl, 2.5 mM CaCl_2), equal to 40 times the mass of the sample. The ASD were transferred into an incubator at 35 °C for 30 min, then removed by lifting the corner using forceps, and held in suspension for 30 s before weighing (W_2). The water absorption capacity was calculated using $\text{WAC} = (W_2 - W_1)/W_1$.

Insulin Release Kinetics. ASD were individually placed inside netwell insert supports, prior to being loaded into six-well plates filled with 1.5 mL of British Pharmacopoeia solution A as the wound exudate simulant.²³ All plates were covered and sealed with parafilm prior to being placed on an orbital shaker rotating at 60 rpm at 35 °C for up to 21 days. Insulin supernatants were measured using a human ELISA assay kit using human recombinant insulin as calibration standard. A cumulative release plot was constructed by adding the quantity of insulin released at each time point and expressing it as a ratio of the total insulin released over time versus the amount of insulin initially encapsulated within the microparticles. Supernatants were replaced with fresh solution A after each sampling.

Cell Culture of HaCaT Cells. HaCaT cells were cultured in T75 flasks containing 10 mL complete DMEM medium supplemented with 10% FBS and 1% pen-strep. Cells were incubated at 37 °C and maintained in an atmosphere of 5% CO_2 . When cells reached 90–95% confluence, the medium was aspirated and cells washed with 15 mL of phosphate-buffered saline (PBS). Cells were then trypsinized with 5 mL of 0.25% trypsin and 1 mmol EDTA solution for 5 min. The trypsin was neutralized with complete media, and cells were centrifuged at 200g for 5 min and then resuspended in 10 mL of fresh complete medium. Cells were counted by removing 10 μL of cell suspension and combining it with an equal volume of trypan blue solution to determine the viable cell count. This mixture was vortexed and a sample loaded into a hemocytometer chamber (Fisher; Pittsburgh, U.S.A.) and cells counted under an inverted microscope (VWR; Mississauga, Canada).

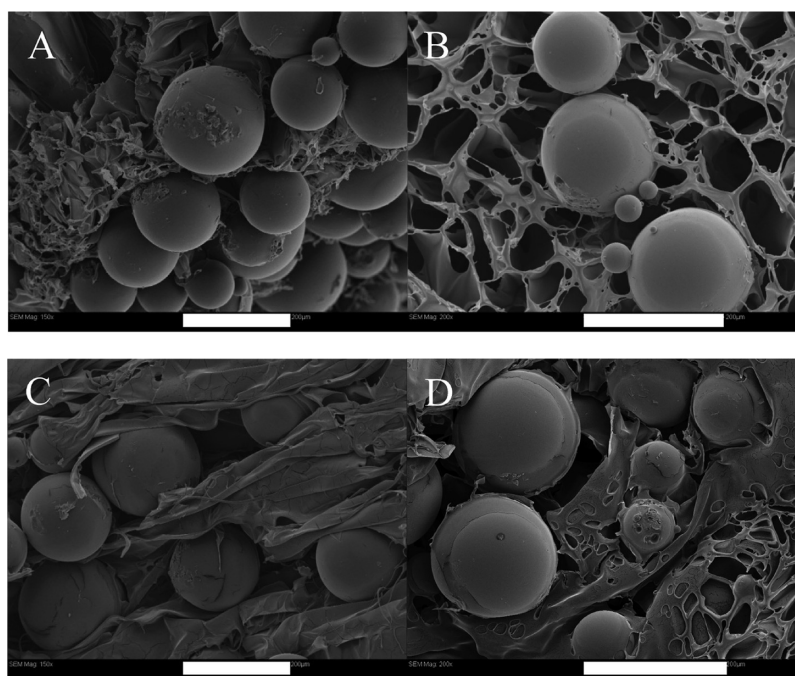


Figure 1. Cross-sectional SEM images of 2% M- (A), 4% M- (B), 2% G- (C), and 4% G- (D) ASD loaded with insulin–PLGA microparticles. White scale bars represent 200 μm .

Insulin Bioactivity: HaCaT Cell Scratch Assay. HaCaT cell suspensions were diluted to 250000 cells/mL in complete growth medium containing 10% FBS and seeded onto 24 well plates (Costar; Lowell, U.S.A.) to a final well volume of 1 mL. Cells were allowed to reach confluency after 48 h, at which time a single scratch was made using the tip of a plastic disposable 10 μL pipet tip. All wells were washed twice with 1 mL of DPBS to remove cellular debris. Then 500 μL of starvation medium consisting of DMEM, 2% FBS, and 1% pen-strep was used to prepare solutions with an insulin concentration of 10^{-7} M from (i) freshly dissolved crystalline insulin and (ii) supernatants with insulin released from alginate dressings containing insulin-loaded PLGA microparticles. Supernatant from blank alginate dressings were also tested as negative controls. In some cases, supernatants contained very little insulin, making it difficult to achieve the 10^{-7} M concentration. The samples that have been affected are indicated in the figure caption. Cell migration across the scratch was measured under a phase contrast inverted microscope (VWR; Mississauga, Canada) at 0, 4, 24, and 48 h.

Statistical Analysis. Statistical analysis was conducted with GraphPad Prism 5. A one-way ANOVA, followed by a pairwise comparison, was performed on scratch assay data, with a $p = 0.05$. All experiments except for the insulin release kinetics were performed using three separate ASD samples tested individually and reported as the mean with standard error. The insulin release kinetics were reported as the mean with standard error of three separate ASD samples plated in duplicate for each individual supernatant.

RESULTS AND DISCUSSION

Wound dressings are important medical devices that help restore the natural integrity of damaged skin. Dressings are designed to achieve several goals including the provision of a moist wound environment to increase healing rates, the improvement of cosmesis and the reduction of pain and infection.^{24,25} Addition of controlled release, wound healing–promoting agents would be an important breakthrough in the design of more effective dressings. Here we have explored the approach of incorporating insulin, a proven promoter of healing, into controlled release microparticles that are, in turn, embedded in a composite, predominantly biopolymer-based,

dressing material. Hydration of the material triggers the controlled, sustained release of bioactive insulin, which in turn should stimulate tissue healing and regeneration based on the results of previous studies.

As a first step in the design of this novel type of active dressing, crystalline insulin was encapsulated into PLGA microparticles that can function as a drug depot device that slowly and controllably delivers bioactive insulin over a 25-day period.¹⁴ The release kinetics can be tailored through adjustment of the quantity of encapsulated insulin. The ability of insulin to stimulate keratinocyte migration is a key factor in accelerating wound closure.²⁶ However, microparticles are difficult to distribute directly in a homogeneous manner and to be retained over a wound surface. In addition, microparticles alone have no capacity to function as a barrier or to provide an optimal, moist wound healing environment. As a result, a polymer matrix with the ability to isolate the wound, and absorb and retain moisture is critical. This would not only be advantageous in providing a moist wound healing environment, but would also drive PLGA hydrolysis and insulin diffusion toward the wound. Likewise, the candidate material could be stored in a dry and stable state when not in use, but should be robust enough to manipulate, and be sufficiently elastic to stretch and conform to the uneven surfaces of the wounded skin. The approach used was to entrap insulin-loaded microparticles into an alginate-PEG sponge dressing matrix, forming a porous, absorbent alginate hydrogel-based sponge dressing when hydrated.

Encapsulation Efficiency. Prior to incorporating insulin-loaded PLGA microparticles into the ASD, the amount of insulin loaded was measured. Three microparticle batches were prepared and the mean crystalline insulin loading of 0.04 mg/mg of microparticle determined, representing an $80 \pm 7\%$ encapsulation efficiency.

Alginate Sponge Dressing Morphology. Strength is a critical component of wound dressing and can be influenced by

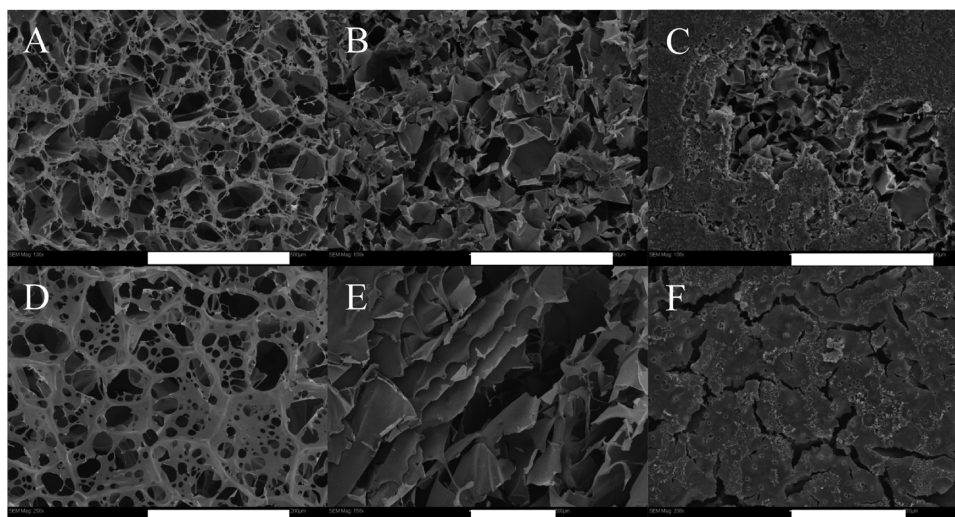


Figure 2. Cross-sectional SEM images of P/M-ASD prepared with 1.45 kDa PEG at concentrations of 0.1 (A), 1 (B), and 10% (C). Images of P/M-ASD with 10 kDa PEG at concentrations of 0.1 (D), 2 (E), and 10% (F). White scale bars in images A–C and D–F represent 500 and 200 μm , respectively.

the morphology and chemical composition of a material. Scanning electron micrographs in Figure 1A–D, revealed a complex, porous microstructure in both M-ASD and G-ASD with clusters of microparticles embedded within the lamellar structure. Distinct differences in morphology were observed between M-ASD (Figure 1A,B) and G-ASD (Figure 1C,D). M-ASD revealed a highly corrugated and sharp lamellar structure with pores having an internal diameter ranging from approximately 6–105 μm . G-ASD, on the other hand, showed smoother, fold-like lamellar structures with the absence of distinct open porous spaces.

ASD prepared with 0.1–10% PEG at a molecular weight 1.45 kDa (Figure 2A–C) or 10 kDa (Figure 2D–F) were also examined using SEM. The dressings with the lowest concentration of 1.45 kDa PEG displayed almost no morphological difference to PEG-free M-ASD, revealing little bulking effect by PEG incorporation. As the PEG concentration increased to 1% (Figure 2B), the corrugated surfaces of the sharp lamellar internal structures became increasingly larger, and an overall bulking effect of the foam network was observed. As the 1.45 kDa PEG content was increased to 10% (Figure 2C), the porous lamellar sponge network became covered by a dense, outer layer of PEG, filling in much of the porous internal spaces.

Figures 2D–F show the effects of incorporating 0.1–10% PEG 10 kDa into high M alginate sponge dressing (P/M-ASD). An immediate bulking effect was apparent with the incorporation of higher molecular weight 0.1% 10 kDa PEG (Figure 2D). The internal lamellar structure supporting the pores appeared bulkier and smoother, with less of a corrugated arrangement than PEG-free M-ASD. As the concentration of 10 kDa PEG increased to 1% the open cell internal structure of the P/M-ASD transitioned into aligned and thick, layered sheets of alginate and PEG (Figure 2E). Finally, as the concentration of 10 kDa PEG increased to 10% (Figure 2F), the internal open cell structures were completely lost and the P/M-ASD became a solid mass.

Scanning electron microscopy revealed that for the most part, both M- and G-ASD had similar, thin reticulating pore microstructures. As more alginate and PEG were added to the formulation, the pore walls became noticeably bulkier in size.

Shapiro et al. (1997) reported that as the overall polymer content of a porous material increases, the additional polymer adds to the bulkiness of the pore walls.²⁷ Alginate and PEG content therefore played a role in contributing to the morphology of the pore walls within ASD.

Density of Sponge Dressings. Densities of ASD are summarized in Table S1. In both, M- and G-ASP, the density doubled in response to a doubling in initial alginate solution concentration from 2–4% in the preparation of the sponge dressing. The effect of adding various concentrations of PEG with different molecular weights into G-ASD (formed with 2% alginate) also had an effect on final ASD density, as shown in Table S2. As PEG concentration increased in P/M-ASD, the density did so as well. PEG molecular weight did not significantly affect the density of the P/M-ASD between 1.45 to 10 kDa.

Tensile Strength of Sponge Dressings. Tensile testing was performed on ASD to determine the influence of alginate type and PEG content on dressing stiffness, an important property that determines how well a dressing can stretch around body contours. Young's modulus (MPa), maximum stress at fracture (MPa), and the percent elongation at fracture of M- and G-ASD made from 2 and 4% alginate solutions are summarized in Table S3. In both M- and G-ASD, the Young's modulus increased with alginate concentration, indicating a stiffer material. On the other hand, the Young's modulus showed no significant difference between M- and G-ASD suggesting that alginate concentration plays more of a role in controlling ASD stiffness, than alginate chemistry. As alginate concentration was increased from 2 to 4%, the tolerated stress before failure increased by about 4-fold. These trends were similar in both M- and G-ASD, indicating that the alginate chemistry played less of a role in governing tensile strength, as opposed to the density, which was a more influencing factor. On the other hand, the percent elongation at fracture remained nearly constant across all four of the different formulations. Considering density and tensile strength, denser ASD proved to be much stiffer, and was not as influenced by the type of alginate used (M or G).

Alternatively, the incorporation of low and high molecular weight PEG at different concentrations was further investigated

to determine if dressing stiffness could be controlled. The effect of PEG molecular weight and concentration on tensile strength is illustrated in Table S4. When 1.45 kDa PEG was introduced to M-ASD, an increase of PEG from 0.1% to 1.0% reduced the Young's modulus from 5.0 to 2.2 MPa, almost half the original value, indicating that PEG had initially increased the Young's modulus in comparison to PEG-free ASD, but then dropped as PEG concentrations surpassed 0.1%. With PEG concentrations increasing beyond 0.1%, the reduction in stiffness of the sponge was a result of PEG's plasticizing effect which increases flexibility and reduces brittleness.²⁸ Beyond 1% 1.45 kDa PEG, the ASD became increasingly PEG-based and too fragile to handle.

The experiment was repeated using P/M-ASD made from 0.1 to 1%, 10 kDa PEG to determine if increasing the molecular weight of PEG could have a more significant effect on reducing the Young's modulus. The result was an immediate reduction in the Young's modulus for preparations containing 0.1 and 1% 10 kDa PEG. The dressings, however, were so delicate, that the calculated moduli were nearly baseline, indicating that, as the molecular weight of PEG increases significantly in P/M-ASD, the material becomes too fragile to be physically stretched. The maximum stress achieved by P/M-ASD containing 10 kDa PEG was nearly zero, indicating that no matter the PEG content, high molecular weight PEG limits any significant amount of stretching. At 10% PEG, P/M-ASD was too brittle to test.

Water Vapor Transmission Rate and Water Absorption Capacity of ASD. Water vapor transmission rate (WVTR) and water absorption capacity (WAC) were determined for 2–4% M- and G-ASD, as summarized in Table S5. M- and G-ASD prepared from solutions of 2% M or G alginates, transmitted between 17 and 18 mg/cm²/h vapor with no significant difference between preparations. WAC of M- and G-ASD measured between 16 and 27 mg H₂O/mg ASD showing a greater capacity to absorb water in ASD prepared with 2% alginate solutions versus 4%. WVTR and WAC were also measured on ASD prepared from solutions of 2% M alginate, combined with 0.1–10% 1.45 and 10 kDa PEG, as reported in Table S6. When 1.45 kDa PEG was introduced into the M-ASD, the WVTR jumped to a range of 23–29 mg/cm²/h, which was slightly higher than ASD without PEG. PEG as a hygroscopic material may be acting as a desiccant, absorbing as opposed to transmitting water vapor through the dressing material. To determine if PEG molecular weight had an effect, samples with 0.1–10% 10 kDa PEG were tested. A similar range of WVTR of 24–29 mg/cm²/h was measured, indicating that increasing the PEG molecular weight had little effect on WVTR.

Because PEG increased WVTR, it was also important to determine if WAC could be controlled by varying the amount and molecular weight of PEG. M-ASD were prepared with 0.1–1.0% 1.45 or 10 kDa PEG, and resulted in a WAC ranging from 15 to 19 mg H₂O/mg ASD. When comparing to PEG-free ASD formulation, PEG reduced the absorptive capacity of the ASD slightly. This effect is due to the reduction in porosity and surface area as the ASD becomes denser, with higher levels of PEG being added to the formulation. Data was unavailable for dressings with 10% PEG because the dressing material dissolved in the assay solution.

Although flexibility and strength are important wound dressing attributes, water absorption and vapor transfer are equally as important. Because human burn wounds can release exudate at a rate of 20 mg/cm²/h, the ability of a wound

dressing to absorb and release moisture through evaporation ensures that the wound is kept moist but not wet.^{29,30} Moisture is also an important driving force in PLGA erosion and the diffusion of insulin, so being able to adjust the formulation to maintain a moist environment is essential. One method of controlling water absorption capacity was by changing the internal sponge surface area. Lower density M- and G-ASD had highly open, complex porous networks that absorbed up to 30 times its mass in water, whereas denser materials absorbed much less water. Although this capability is important, especially in wounds with heavy exudate, retaining such large amounts of moisture can also promote bacterial growth and impede healing. Quinn et al. (1985) recommended that water vapor transfer rates for burn wound dressings should range between 8 and 10 mg/cm²/h to sustain healthy healing.⁵ In the present study, M-, G-, and P/M-ASD exhibited WVTR values that were nearly double and triple the recommended range. Although this may suggest that the wound could dry out, a secondary dressing used to secure the ASD in place over the wound could also function to reduce the rate of moisture loss.³¹ The formulation studies have therefore demonstrated that polymer content is an important contributor to sponge density, which in turn influences flexibility, strength, and water handling properties.

Insulin Release Kinetics. Insulin release kinetics were plotted in Figure 3 for M- and G-ASD containing 5 mg of

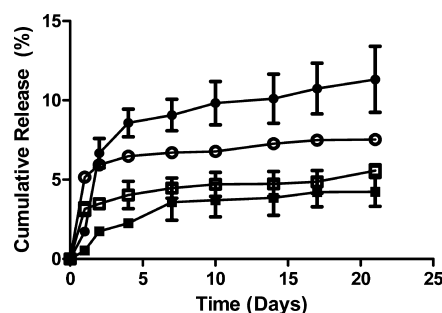


Figure 3. Insulin release kinetics from ASD prepared from 2% (-○-) and 4% (-●-) M and 2% (-□-) and 4% (-■-) G alginates.

insulin-loaded PLGA microspheres. Over 21 days of assay, M-ASD released a cumulative 6–12% of the entrapped insulin, whereas G-ASD released 3–5% of the encapsulated insulin. After the initial release, M- and G-ASD provided insulin sustained release over the following 21 days. M-ASD appeared to maintain near zero order release kinetics over the assay period, more so than G-ASD, which plateaued earlier.

Figure 4 is a plot of insulin released from P/M-ASD prepared with 0.1–10% 1.45 or 10 kDa PEG. All P/M-ASD released approximately 20–30% of the total entrapped insulin over a 21 day period. Almost no immediate release of insulin was observed in any of the P/M-ASD, as opposed to the PEG-free ASD. Near zero order release kinetics were maintained until day 14, after which the release kinetics gradually plateaued. Differences in PEG molecular weight and content did not appear to play a role in P/M-ASD release beyond 14 days, however, significantly improved the amount of insulin detected over the entire study period when compared to PEG-free ASD. This effect is likely to be the result of PEG's ability to stabilize proteins in solution³² and also promote a shift in equilibrium toward the liberation of monomeric forms of the insulin from

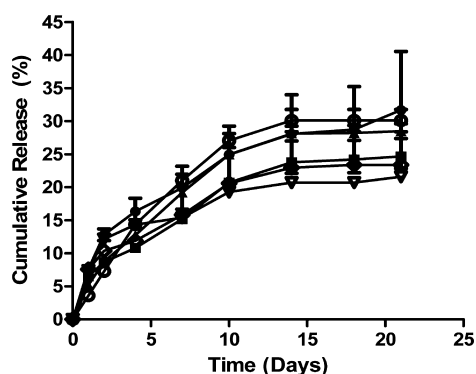


Figure 4. Insulin release kinetics from ASD prepared from 2% M alginate solution with 0.1% (●), 1% (■), and 10% (▲) 1.45 kDa PEG and 0.1% (▽), 1% (◇), and 10% (○) 10 kDa PEG.

multimeric configurations,³³ which are stoichiometrically quantifiable with the ELISA assay.

Insulin release kinetics were considered over a 21 day period, a time frame critical for wound healing. ASD with and without PEG released nearly equivalent amounts of insulin within the first 24 h. Because all formulations contained the same amount of insulin–PLGA microparticles, it is possible that the surface bound insulin was first to dissolve in equivalent proportions. After 5 days, differences in the release kinetics began to appear in PEG-free ASD, which resulted in less insulin being released over the same period of 25 days. Although the acidic degradation products of PLGA were considered as potentially responsible for reduced insulin release, previous study demonstrated that biologically active insulin was released from PLGA for an extended period of 25 days as verified through two assays.¹⁴ One assay showed high activity of released insulin through the stimulation of rat L9 myoblasts, phosphorylating Akt. The second assay, similar to that used in this study, involved measuring HaCaT cell migration following an applied injury to a cell monolayer. As such, insulin-PLGA microparticles embedded within ASD provide a convenient and effective method of delivering detectable levels of insulin over a month-long period of time.

Bioactivity of Released Insulin: HaCaT Scratch Assay.

Wounding experiments were simulated using a cell monolayer scratch assay with a human keratinocyte cell line (HaCaT) to assess the bioactivity of released insulin. A scratch of

approximately 500 μm in width was made on a confluent layer of HaCaT cells and monitored for the progression of cell migration upon stimulation with insulin. Figure 5 shows a representation of (A) HaCaT cells after being freshly scratched and (B) recovery after 48 h. Figures 6 and 7 show the extent of

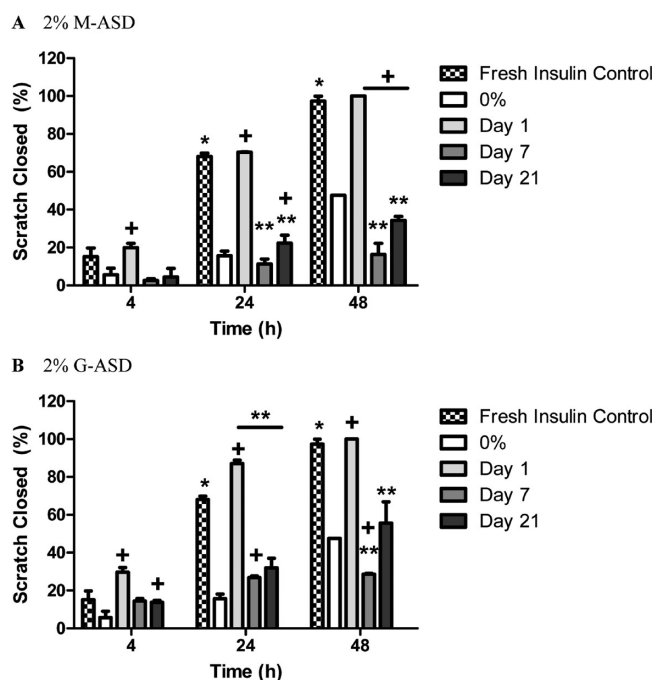


Figure 6. HaCaT cell scratch assays evaluating bioactivity of insulin released from 2% M- (A) and 2% G- (B) ASD from days 1, 7, and 21. *Statistical significance between fresh insulin control and insulin free PLGA supernatant, **Difference between insulin released to supernatant and fresh insulin control, and +difference between insulin released to supernatant and insulin-free PLGA supernatant ($p = 0.05$). Supernatants from days 7 and 21 in (A) and (B) represent samples in which 10^{-7} M insulin was difficult to achieve.

HaCaT cell migration over time to close the scratch, after stimulation. In cases where PEG was used to make up the dressing material, only dressings with 1% PEG were selected.

The greatest stimulation of cell migration took place between 4 and 24 h for cells that were exposed to 10^{-7} M fresh insulin versus the blank control. By 24 h, the scratch was 70% closed

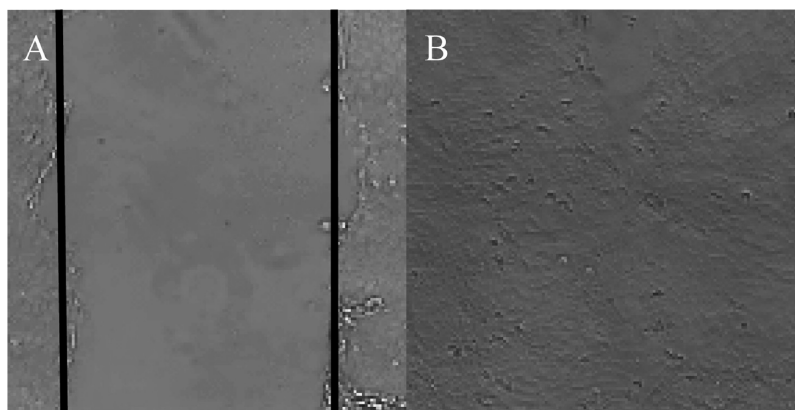


Figure 5. Representation of HaCaT cells after being (A) freshly scratched by a pipet tip and (B) after treatment with insulin for 48 h, as seen through an inverted contrast microscope. The black vertical bars in (A) indicate the margins of the scratch approximately 500 μm in width, with the space between the bars representing the “scratch wound”.

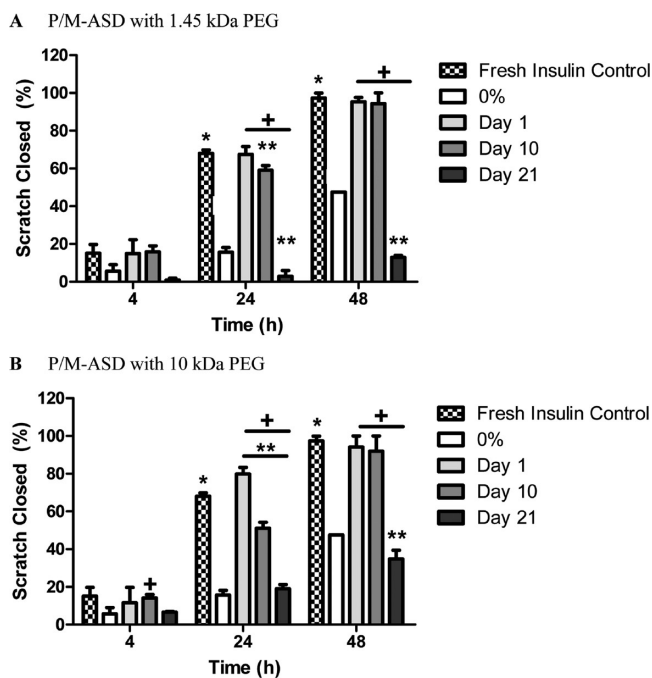


Figure 7. HaCaT cell scratch assays evaluating bioactivity of insulin released from 2% M- with 1% PEG 1.45 kDa (A), and 2% M- with 1% PEG 10 kDa (B) ASD from days 1, 10, and 21. *Statistical significance between fresh insulin control and insulin-free PLGA supernatant; **difference between insulin released to supernatant and fresh insulin control; and +difference between insulin released to supernatant and insulin-free PLGA supernatant ($p = 0.05$). Supernatant from day 21 in (A) and (B) represents samples in which 10^{-7} M insulin was difficult to achieve.

and fully confluent after 48 h, whereas the blank insulin-free negative control failed to achieve full scratch closure in the same period of time. Although some cell migration was observed, cells treated with blank supernatant only reached 15 and 48% scratch recovery at 24 and 48 h, respectively. A one-way ANOVA followed by a pairwise comparison indicated a significant difference between the fresh insulin control and blank alginate control beyond hour 4, suggesting that insulin has a strong stimulatory effect on the migration of HaCaT cells.

A comparison between insulin released from ASD over a 21 day period and fresh insulin is also presented in Figures 6 and 7. In all preparations, insulin released after the first day had the same bioactivity as that of the fresh insulin control and did not differ in performance statistically, over the 48 h scratch assay. When examining the bioactivity of insulin released from M- and G-ASD (Figure 6A,B), both had reduced bioactivity by day 7 of release. In either case, supernatants obtained from day 7 only led to a scratch recovery of 16 and 29% for M- and G-ASD, respectively. By day 21, the bioactivity of the insulin released from M- and G-ASD had similar activity to the blank, only recovering 34% and 56% of the scratch respectively. A comparison between M- and G-ASD revealed that over the course of the scratch assay, insulin bioactivity was similar for both formulations.

ASD prepared from initial solutions of 2% M ASD with 1% 1.45 or 10 kDa PEG had prolonged bioactivity of released insulin for at least 10 days, longer than that of insulin from M- or G-ASD alone (Figure 7 A,B). Insulin bioactivity measured on the first day of the assay was nearly identical for 1.45 and 10 kDa P/M-ASD and comparable to that of the fresh insulin

control. On day 10, however, P/M-ASD supernatants were better able to match the insulin bioactivity comparable to that of the fresh insulin control, as opposed to M- and G-ASD containing no PEG. By day 21, insulin bioactivity had diminished and was inactive as compared to the fresh insulin control.

Overall, insulin bioactivity was maintained for at least 10 days. ASD prepared from 2% M alginate solutions with 1% PEG 1.45 and 10 kDa helped to maintain insulin bioactivity at levels similar to that of fresh insulin versus insulin-free ASD. No differences were observed in activity between P/M-ASD prepared with either 1.45 and 10 kDa PEG.

A cell scratch assay to test insulin for bioactivity is based on the ability to promote changes in cell migration, thus, serving as an in vitro model of repair in human epidermal cells. Insulin released from both M- and G-ASD had strong stimulatory effects after the first day of release, similar to that of the fresh insulin control. However, by day 7 and beyond, the bioactivity was reduced relative to the fresh insulin control. Because low quantities of insulin were being detected during the latter half of the assay, there were often insufficient levels of insulin to reach target concentrations to fully stimulate HaCaT migration. Furthermore, this low concentration of insulin in the supernatants also resulted in HaCaT cells being almost entirely exposed to release solution A, which lacks many of the nutrients normally obtained from the starvation media to facilitate migration and normal growth. On the other hand, the presence of PEG in P/M-ASD sustained insulin bioactivity for up to 10 days. PEG hydrogels have been shown to protect and preserve peptides in harsh environments.³⁴ It also appeared that the PEG molecular weight within the dressing does not influence insulin bioactivity, while its presence is necessary to preserve dressing integrity and insulin bioactivity.

CONCLUSIONS

A variety of factors were examined that can influence the physical properties of ASD that result in increased capability of sustained and controlled release of bioactive insulin. The relationship between polymer content and sponge density revealed that ASD formulated with 2% M-alginate and 1% 1.45 kDa PEG yielded porous sponges with favorable flexibility and water handling characteristics necessary for wound dressings. Insulin was released from these dressings for up to 21 days while maintaining bioactivity for up to 10 days and potentially longer, with the addition of a small quantity of PEG. In conclusion, we have developed an M-alginate-PEG sponge dressing (P/M-ASD) containing PLGA insulin-loaded micro-particles that deliver bioactive insulin in a sustained and controlled manner over a prolonged period of time. This dressing has the potential to be used for the treatment of burn wounds as well as other wounds that have impaired healing.

ASSOCIATED CONTENT

Supporting Information

Tables S1–S6, which highlight the ASD densities, tensile strength, and water handling properties. This material is available free of charge via the Internet at <http://pubs.acs.org>.

AUTHOR INFORMATION

Corresponding Author

*E-mail: neufeld@queensu.ca. Tel.: (613) 533-2827. Fax: (613) 533-6637.

Notes

The authors declare no competing financial interest.

ACKNOWLEDGMENTS

We acknowledge the Natural Sciences and Engineering Research Council of Canada for financial support and for a postgraduate scholarship to M.H. We thank Mr. Charlie Cooney for his assistance with the scanning electron microscopy, Prof. Myron Szewczuk of Queen's University for providing access to cell culture facilities, and Dr. Yan Liu (Burn Department, Ruijin hospital, Shanghai JiaoTong University Medical School, Shanghai, PR China) for comments on the manuscript.

REFERENCES

- (1) Velnar, T.; Bailey, T.; Smrkoli, V. *J. Int. Med. Res.* **2009**, *37*, 1528–1542.
- (2) Palao, R.; Monge, I.; Ruiz, M.; Barret, J. P. *Burns* **2010**, *36*, 295–304.
- (3) Winter, G. D. *Nature* **1962**, *193*, 293–294.
- (4) Field, F. K.; Kerstein, M. D. *Am. J. Surg.* **1994**, *167*, 2S–6S.
- (5) Quinn, K. J.; Courtney, J. M.; Evans, J. H.; Gaylor, J. D. S.; Reid, W. H. *Biomaterials* **1985**, *6*, 369–377.
- (6) Tanaka, A.; Nagate, T.; Matsuda, H. *J. Vet. Med. Sci.* **2005**, *67*, 909–913.
- (7) Puolakkainen, P. A.; Twardzik, D. R.; Ranchalis, J. E.; Pankey, S. C.; Reed, M. J.; Gombotz, W. R. *J. Surg. Res.* **1995**, *58*, 321–329.
- (8) Judith, R.; Nithya, M.; Rose, C.; Mandal, A. B. *Life Sci.* **2010**, *87*, 1–8.
- (9) PeptoTech Inc.. https://www.peprotech.com/en-US/_layouts/PeptoTech/splash.aspx (accessed Jul 11, 2011).
- (10) King, L.; Kennaway, E. L.; Piney, A. *J. Physiol.* **1928**, *66*, 400–402.
- (11) Rosenthal, S. P. *AMA Arch. Surg.* **1968**, *96*, 53–55.
- (12) Udupa, K. N.; Chansouria, J. P. *N Br. J. Surg.* **1971**, *58*, 673–675.
- (13) Liu, Y.; Petreaca, M.; Martins-Green, M. *J. Cell. Mol. Med.* **2009**, *13*, 4492–4504.
- (14) Hrynyk, M.; Martins-Green, M.; Barron, A. E.; Neufeld, R. *J. Int. J. Pharm.* **2010**, *398*, 146–154.
- (15) Segal, H. C.; Hunt, B. J.; Gilding, K. *J. Biomater. Appl.* **1998**, *12*, 249–257.
- (16) Hom, D. B.; Adams, G.; Koreis, M.; Maisel, R. *Otolaryngol.—Head Neck Surg.* **1999**, *121*, 591–598.
- (17) Rowley, J. A.; Madlambayan, G.; Mooney, D. J. *Biomaterials* **1999**, *20*, 45–53.
- (18) Gilchrist, T.; Martin, A. M. *Biomaterials* **1983**, *4*, 317–320.
- (19) Lin, C.; Anseth, K. *Pharm. Res.* **2009**, *26*, 631–643.
- (20) Balakrishnan, B.; Mohanty, M.; Umashankar, P. R.; Jayakrishnan, A. *Biomaterials* **2005**, *26*, 6335–6342.
- (21) Chiu, C. T.; Lee, J. S.; Chu, C. S.; Chang, Y. P.; Wang, Y. J. *Mater. Sci: Mater. Med.* **2008**, *19*, 2503–2513.
- (22) *British Pharmacopoeia 1994*; British Pharmacopoeia Commission, Secretariat of the Medicines and Healthcare Products Regulatory Agency: London, U.K., 1994.
- (23) *British Pharmacopoeia 1995*; British Pharmacopoeia Commission, Secretariat of the Medicines and Healthcare Products Regulatory Agency: London, U.K., 1995.
- (24) Ovington, L. G. *Clin. Dermatol.* **2007**, *25*, 33–38.
- (25) Queen, D.; Evans, J. H.; Gaylor, J. D.; Courtney, J. M.; Reid, W. H. *Burns Incl. Therm. Inj.* **1987**, *13*, 218–228.
- (26) Liu, Y.; Petreaca, M.; Yao, M.; Martins-Green, M. *BMC Cell Biol.* **2009**, *10*, 1–15.
- (27) Shapiro, L.; Cohen, S. *Biomaterials* **1997**, *18*, 583–590.
- (28) Livnat, M.; Beyar, R.; Seliktar, D. *J. Biomed. Mater. Res., Part A* **2005**, *75*, 710–722.
- (29) McColl, D.; Cartlidge, B.; Connolly, P. *Int. J. Surg.* **2007**, *5*, 316–322.
- (30) Mi, F. L.; Wu, Y. B.; Shyu, S.; Schoung, J. Y.; Huang, Y. B.; Tsai, Y. H.; Hao, J. Y. *J. Biomed. Mater. Res., Part A* **2002**, *59*, 438–449.
- (31) Seaman, S. *J. Am. Podiatr. Med. Assoc.* **2002**, *92*, 24–33.
- (32) Novaes, L. C. D.; Mazzola, P. G.; Pessoa, A.; Penna, T. C. V. *Biotechnol. Prog.* **2010**, *26*, 252–256.
- (33) Thurow, H.; Geisen, K. *Diabetologia* **1984**, *27*, 212–218.
- (34) Peppas, N. A. *Curr. Opin. Colloid Interface Sci.* **1997**, *2*, 531–537.